SHAPE, SPIN, STRENGTH, AND STABILITY OF BENNU. J.H. Roberts[1], O.S. Barnouin[1], G.A. Neumann[2], M.C. Nolan[3], M.E Perry[1], R.T. Daly[1], C.L. Johnson[4,5], M.M. Al Asad[4], M.G. Daly[6], E.E. Palmer[5], J.R. Weirich[5], K.J. Walsh[7], D.J. Scheeres[8], J.W. McMahon[8], D.S. Lauretta[3], [1]The Johns Hopkins University Applied Physics Laboratory, Laurel, MD, USA; [2]NASA Goddard Space Flight Center, Greenbelt, MD, USA; [3]Lunar and Planetary Laboratory, University of Arizona, Tucson, AZ, USA; [4]Department of Earth, Ocean and Atmospheric Sciences, University of British Columbia, Vancouver, Canada; [5]Planetary Science Institute, Tucson, AZ, USA; [6]The Centre for Research in Earth and Space Science, York University, Toronto, Ontario, Canada; [7]Southwest Research Institute, Boulder, CO, USA; [8]Colorado Center for Astrodynamics Research, University of Colorado, Boulder, CO, USA.

Introduction: Images of asteroid (101955) Bennu acquired by the OSIRIS-REx mission [1,2] reveal a rocky world covered in rubble, including numerous boulders with diameters up to tens of meters. The geologic evolution of Bennu is driven in large part by downslope migration of surface material [3] and rubble, which may be dislodged from an initial state by a number of processes, such as YORP-induced spin-up [4,5], re-accumulation [6,7], impact-induced seismic shaking, thermal stresses, or tidal disruption by close encounters with larger bodies.

Shape: Shape models of Bennu have been developed from images using stereophotoclinometry (SPC) [8] and from lidar data collected by the OSIRIS-REx Laser Altimeter (OLA) [9,10]. A SPCOLA shape model derived from a combination of both datasets is shown in Figure 1. A spherical harmonic decomposition of the shape (Figure 2) reveals a number of interesting features, which can be used to interpret the geological significance of the shape. The zonal terms show a sharp dichotomy between the odd and even terms, which is indicative of symmetry about the equator. These zonal terms also are particularly strong at degrees 2 and 4. Figure 3a,b shows a reconstruction of the SPCOLA shape model from the spherical harmonics, truncated at degree 4. The zonal component at degree-4 is largely due to the equatorial ridge typical of top-shaped asteroids, and the strong sectoral component reflecting high-

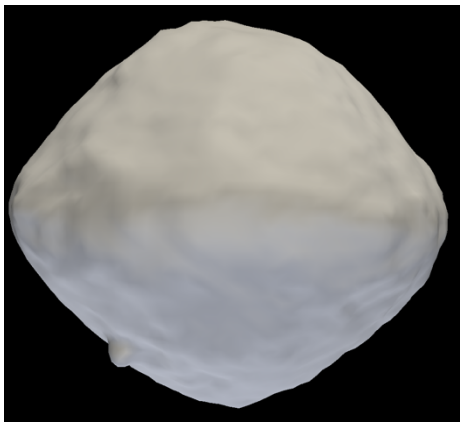

Figure 1: SPCOLA Shape model (v34) shown at 12-m resolution.

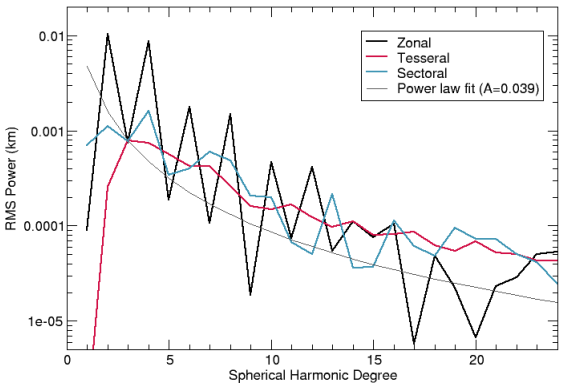

Figure 2: Spherical Harmonic decomposition of Bennu's global topography.

standing longitudinal ridges, which are most obvious as a "squarish" outline as viewed from the poles [10].

Figure 3c,d extends the reconstruction out to degree-8, to show the next level of detail. The next pair of spikes shown in the zonal terms at degrees 6 and 8 in Figure 2, are indicative of the terraces (Barnouin et al., 2019). The larger craters are noticeable in the degree-8 shape model as well. We also note that the tesseral terms decay much more slowly than the Vening-Meinesz style power law [11] would predict, suggesting the fractal nature of the size distribution of the surface of the rubble.

Internal properties: The large-scale surface topography may also provide insight as to the strength of the interior. Although Bennu appears to be an unconsolidated rubble-pile asteroid, it cannot be completely strengthless because the shape deviates from a hydrostatic surface. Indeed, there is no hydrostatic shape that is consistent with Bennu's observed rotation rate and density, and it must be supported either by internal friction or cohesion. In the absence of cohesion, an angle of internal friction of 18° is necessary to maintain the current shape against large-scale failure, flattening, and potential disruption (Figure 4) [10]. This could also be achieved by ~ 1 Pa of cohesion [12].

Stability: Previous analysis of the shapes and spins of small bodies indicate that these properties will gradually evolve towards a condition of maximum topographic stability; that is, a state of low topographic variation, low slopes, and low surface erosion (mass-

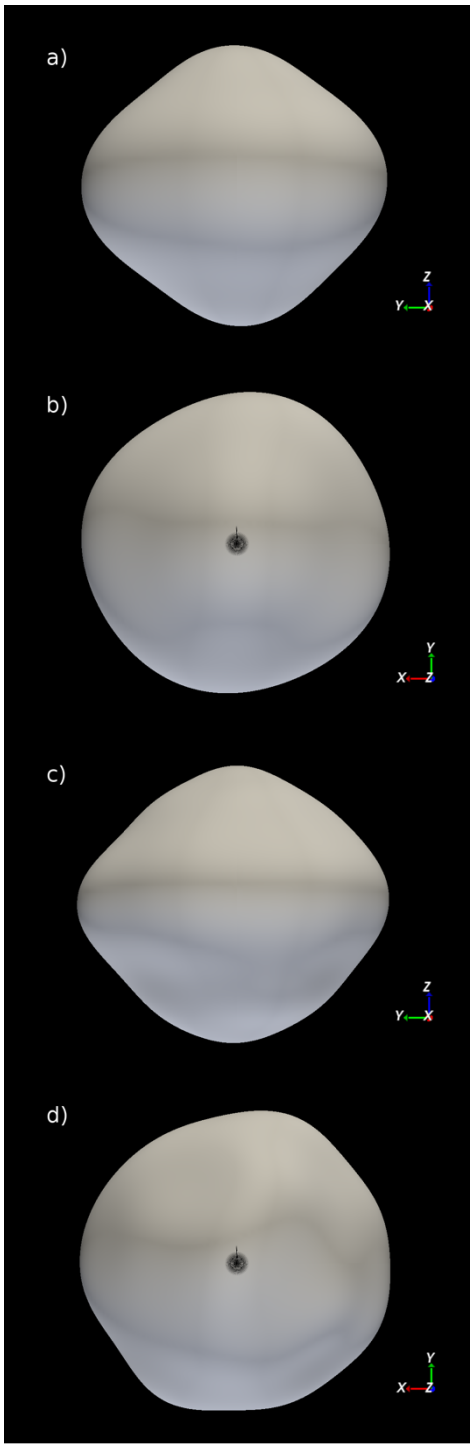

Figure 3: Reconstructions of SPCOLA shape model out to degrees 4 (a,b) and 8 (c,d) viewed from the equator (a,c) and north pole (b,d). Pole indicated by black circle.

wasting) rates. However, Bennu is already rotating faster than the optimum rate for this stability condition, and the YORP effect is further increasing the rotation rate. Rotational stability analysis demonstrates that an internal friction angle of at least 18° is necessary to

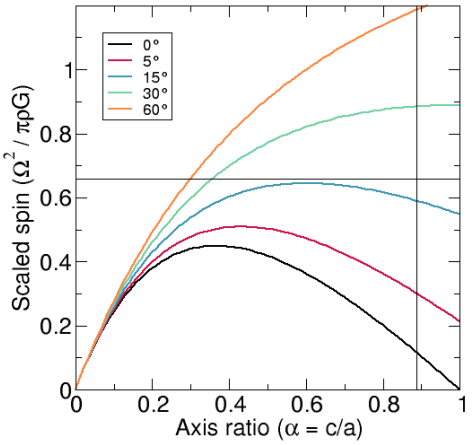

Figure 4: Maximum stable spin rates as a function of the oblateness of the body for various angles of internal friction (without cohesion). Bennu's rotation rate and shape are indicated by the solid lines.

prevent Bennu from failure via mass wasting in the absence of cohesion. However, if the observed increase in rotation rate [12] persists, in less than 0.6 Myr, no amount of internal friction would be sufficient to prevent failure. and significant cohesion (>15 Pa) would be required. We note that catastrophic disruption due to YORP spin-up is extremely unlikely. As the asteroid begins to deform, the increased oblateness results in a higher moment of inertia, and would cause the asteroid to spin down, potentially moving it into a stable regime. Moreover, YORP can change on short timescales, and is very sensitive to the precise shape of the body. Thus, the deformation of the asteroid may be halted after a small episode of failure. A more comprehensive evolution of the deformation and spin rate [13] is under investigation.

Acknowledgements: This material is based upon work supported by NASA under Contract NNM10AA11C issued through the New Frontiers Program. We are grateful to the entire OSIRIS-REx Team for making the encounter with Bennu possible.

References: [1] DellaGiustina, D. N. et al. (2019) Nat. Astron. 3, 341–351. [2] Walsh, K.J. et al. (2019) Nat. Geosci. 12, 242–246. [3] Richardson, J.E. and Bowling, T.J. (2014) Icarus 234, 53–65. [4] Rubincam, D.P. (2000) Icarus, 148, 2–11. [5] Walsh, K.J., et al. (2008) Nature, 454, 188–191. [6] Michel, P. et al. (2001) Science, 294, 1696–1700. [7] Michel, P. et al. (2019) LPSC 50, 1659. [8] Gaskell, R.W. et al. (2008) MAPS, 43, 1049–1061. [9] Daly, M.G. et al. (2017) SSR, 212, 899–924. [10] Barnouin, O.S. et al. (2019), Nat. Geosci., 12, 247–252. [11] Bills, B.G. and Kobrick, M. (1985) J. Geophys. Res. 90, 827–836. [12] Scheeres, D. J. et al. (2019) Nature Astron. 3, 352–361. [13] Cotto-Figueroa, D. et al. (2015) ApJ 803, 25.